

Elsevier required licence: © 2018. This manuscript version is made available under the CC-BY-NC-ND 4.0 license
<http://creativecommons.org/licenses/by-nc-nd/4.0/>

Spectroscopic characteristics of dissolved organic matter from aquaculture wastewater and its interaction mechanism to chlorinated phenol compound

Linxian Huang ^a, Meilin Li ^a, Huu Hao Ngo ^b, Wenshan Guo ^b, Weiyong Xu ^a, Bin Du ^a, Qin Wei ^c, DongWei ^{a,*}

^a School of Resources and Environment, University of Jinan, Jinan 250022, PR China

^b School of Civil and Environmental Engineering, University of Technology Sydney, Broadway, NSW 2007, Australia

^c Key Laboratory of Interfacial Reaction & Sensing Analysis in Universities of Shandong, School of Chemistry and Chemical Engineering, University of Jinan, Jinan 250022, PR China

* Corresponding author. E-mail address: weidong506@163.com (D.Wei).

Abstract

In present study, the characteristics of dissolved organic matter (DOM) from aquaculture wastewater and its interaction to 4-chlorophenol (4-CP) was evaluated via a spectroscopic approach. According to EEM-PARAFAC analysis, two components were derived from the interaction samples between DOM and 4-CP, including humic-like and fulvic-like substances for component 1 and protein-like substances for component 2, respectively. The fluorescence intensity scores of two PARAFAC-derived components decreased with increasing 4-CP concentration. Synchronous fluorescence coupled to two-dimensional correlation spectroscopy (2D-COS) implied that DOM fractions quenched different degrees and occurred in the order of fulvic-like and humic-like fractions > protein-like fraction. Moreover, the quenching mechanisms were mainly caused by static quenching process. It was also found from Fourier transform infrared spectroscopy that the main functional groups for interaction between 4-CP and DOM were O–H stretching and C=O stretching vibration. The obtained results provided a spectroscopic approach for characterizing the interaction between organic pollutant and DOM from aquaculture wastewater.

Keywords: Dissolved organic matter (DOM); 4-Chlorophenol; Excitation-emission matrix (EEM); Synchronous fluorescence spectra; Two-dimensional correlation spectroscopy (2D-COS)

1. Introduction

Aquaculture, as the farming of fish, shellfish and aquatic plants, has been practiced for thousands of years in natural, marine and freshwater environments etc. [1,2]. As a global scale of food economy, it has been growing steadily in developing countries and regions in the past decades. However, large quantities of wastewaters, including dissolved organic matter (DOM), nitrogen- and phosphorus-compounds etc., have been discharged into freshwater due to the rapid growth of aquaculture farms and thus cause significant decline of quality of receiving water and reclaimed water [3].

DOM is a well-known heterogeneous mixture of complex organic compounds with different molecular sizes, structures, and chemical properties [4]. The main compositions in DOM are

consisted of polysaccharide (PS), protein (PN), lipids and humic substances etc., each of which contains abundant functional groups and active sites to interact with organic pollutants [5]. There is increasing evidence that the interaction between DOM and organic pollutants could significantly affect the speciation, solubility, mobility, toxicity and ultimate fate of organic pollutants in aquatic environment [6]. As one type of toxic organic pollutants, chlorinated phenol compounds have been widely applied in the production of pesticides, herbicides, and wood preservatives etc. [7]. Especially, 4-chlorophenol (4-CP) is widely existed in soil, sediment, and water as by-products of pulp and paper, dyestuff, pharmaceutical and agrochemical industries [8]. Therefore, it is of great significance to research the interaction between DOM and 4-CP in order to better understand the fate and biogeochemistry cycling of chlorinated phenol compounds.

At present, a wide range of techniques have been used to evaluate the interaction mechanism between DOM and organic pollutants, such as UV-vis, high-performance liquid chromatography (HPLC), molecular weight distribution, fluorescence spectroscopy and molecular modeling etc. [9,10]. Among all above techniques, fluorescence spectroscopy has been widely utilized as a feasible technique for molecular structure assessment of DOM because of its sensitivity and selectivity. Compared with conventional two-dimensional scan mode, three-dimensional excitation-emission matrix (3D-EEM) could provide more insightful information about both fluorescent intensity and fluorescent location by changing excitation wavelength and emission wavelength simultaneously [11]. In particular, parallel factor analysis (PARAFAC), as a multivariate data analysis technique, has been successfully used for providing the additional quantitative information for describing the distribution of independent fluorescent components in EEM spectra [12]. Till now, the combination of EEM-PARAFAC model has been well applied to quantitative analysis of different fluorescent substances in various environmental samples. He et al. [13] characterized DOM humification by using EEM-PARAFAC and fluorescence regional integration analysis, suggesting that the volume ratio between humic-like and protein-like regions can be used to evaluate humification. Ni et al. [14] characterized, fractionized, and quantified soluble microbial products (SMP) in activated sludge treatment process, identifying two components in SMP samples by using integrated EEM-PARAFAC and mathematical approach. However, it is accepted that various active sites are coexisted in the main compositions of DOM, and thus supply different interaction abilities in influencing organic pollutant [15]. It is insufficient from EEM-PARAFAC analysis about the sequence of interaction abilities between different DOM components and organic pollutant.

At present, two-dimensional correlation spectroscopy (2D-COS) has been well developed to solve the above-mentioned problem by probing the specific sequence of spectral intensity changes corresponding to external perturbations [16,17]. To date, the application of 2D-COS coupled to synchronous fluorescence spectra has been successfully used to evaluate the interaction between various types of fluorescent matters and pollutant in the environmental field. Synchronous fluorescence spectroscopy is a rapid, sensitive and nondestructive method to analyze the micro-environmental changes of chromophores through simultaneously scanning excitation and emission wavelengths [18]. Wei et al. [19] evaluated extracellular polymeric substances (EPS, one kind of microbial products) for Zn(II) interaction during sorption process by using 2D-COS, suggesting that protein-like substances were more susceptible to Zn(II) interaction than that of humic-like substances. Xu and Jiang [17] found that the photodegradation of organic matters associated with

cyanobacterial blooms followed the sequence of tyrosine-like > humic like > tryptophan-like substances. Therefore, it is postulated that the combination of 2D-COS could further supply the interaction sequence between chlorinated phenol compound and DOM at molecular-scale, which is better to understand the behavior and impact of organic pollutant in aquaculture system.

Herein, a spectroscopic approach was applied to characterize the interaction mechanism between DOM from aquaculture wastewater and 4-CP. To achieve this purpose, a combination of 3D-EEM, PARAFAC, synchronous fluorescence spectra, 2D-COS and Fourier transform infrared spectroscopy (FTIR) were used to comparatively evaluate DOM and 4-CP interaction process. The result derived from this study could be helpful to understand the fate of chlorinated phenol compounds in aquaculture environment in the presence of DOM.

2. Materials and methods

2.1. Source of aquaculture wastewater

Sample of aquaculture wastewater was collected from a small-scale fish farm in July, located at Jinan, Shandong province. This kind of small fish farm is commonly found in developing country of China. Moreover, the activity of fish and microorganism in summer are relatively high due to the hot temperature, which may cause higher DOM release into the environment. A total of 4 samples were collected from the four corners of fish farm. After mixed the 4 samples together, the mixed solution was filtered through a 0.45 nm filter, and next stored at 4 °C until use. The raw pH value and total organic carbon (TOC) of mixed DOM from aquaculture wastewater were about 7.5–7.7 and 16.0 ± 0.007 mg/L ($n = 3$), respectively. The PS and PN concentrations in DOM were 24.1 ± 0.28 and 19.2 ± 0.33 mg/L ($n = 3$), respectively.

2.2. Fluorescence quenching titration

The interaction between raw DOM and 4-CP was investigated by using fluorescence quenching titration experiment. More detailed, 25 mL of DOM solution was added with a series volume of pre-determined 4-CP solution (100 mg/L) in a 50 mL volumetric flask. The final 4-CP concentrations in mixed solution were successively varied from 0 to 5 mg/L. The initial pH was adjusted to 7.0 by using 0.1 mol/L HCl or NaOH, as similarly reported by Sheng et al. [20]. Afterwards, the solution was mixed with oscillator for 12 h to ensure equilibrium before spectra measurement at 25 °C. A total of 8 dose-dependent fluorescence spectra could be obtained.

2.3. EEM-PARAFAC

3D-EEM spectra of DOM samples were measured by using a luminescence spectrometer (LS-55, Perkin-Elmer Co., USA), and collected by subsequent scanning emission from 280 to 550 nm at 0.5 nm increments by varying the excitation wavelength from 200 to 400 nm at 10 nm increments. The width of the excitation/emission slit and scanning speed were set to 10.0 nm and 1200 nm/min, respectively. PARAFAC analysis was conducted by using Matlab 7.0 (Mathworks, Natick, MA) with N-way box to extract fluorescent components from EEM fluorescence data [21]. Core consistency diagnostic was applied to determine the correct numbers of components.

2.4. Synchronous fluorescence coupled with 2D-COS

Synchronous fluorescence spectra of DOM were measured through simultaneous scanning the excitation and emission wavelength from 250 to 550 nm with a constant offset ($\Delta\lambda$) of 60 nm [22]. In this study, the increased dosage of 4-CP was selected as the external perturbation, and thus a set of dosage-dependent fluorescence spectra were obtained. 2D-COS was applied to investigate the change of synchronous fluorescence spectra through extending the spectra along the second dimension. The synchronous and the asynchronous 2D spectra could be obtained from the method reported by Noda [23]. The mathematical expressions of the two types of maps are expressed as follows:

$$\Phi(x_1, x_2) = \frac{1}{T_{\max} - T_{\min}} \int_T^{T_{\max}} \tilde{y}(x_1, t) \cdot \tilde{y}(x_2, t) dt \quad (1)$$

$$\Psi(x_1, x_2) = \frac{1}{T_{\max} - T_{\min}} \int_T^{T_{\max}} \tilde{y}(x_1, t) \cdot \tilde{z}(x_2, t) dt \quad (2)$$

where Φ and Ψ are synchronous 2D and asynchronous 2D spectra, respectively. The parameters of x and t are a spectral variable (i.e., wavelengths) and an external perturbation, respectively. $\tilde{y}(x, t)$ is the dynamic spectrum, and $\tilde{z}(x, t)$ is the Hilbert-transformed orthogonal spectrum.

3. Results and discussion

3.1. 4-CP interaction to DOM determined by EEM-PARAFAC

Fig. 1 shows the 3D-EEM spectra of DOM samples interaction to various dosages of 4-CP. It was observed that the interaction between 4-CP and DOM affected the EEM spectra not only fluorescent peak locations but also peak intensities. Four main fluorescence peaks were identified from the EEM of raw DOM sample (Fig. 1A). Peak A and Peak B were identified at excitation/emission wavelengths (Ex/Em) of about 270/370 nm and 220/351.5 nm, which were assigned to tryptophan protein-like substances and aromatic protein-like substances, as similarly reported by Chen et al. [24]. Peak C and Peak D were identified at Ex/Em of 330/411.5 nm and 240/407 nm, which were related to humic-like and fulvic-like substances, respectively [25]. In general, fluorescence intensities of above peaks in DOM expressed a marked decrease with different degrees after interaction to 4-CP. Additionally, Peak A decreased the maximum value in response to the addition of various dosages of 4-CP, suggesting that aromatic protein-like substances had a large quenching effect in the presence of 4-CP. Similar observation has been reported by Zhang et al. [26], who found that protein-like substances in EPS were significantly quenched as the main fluorescent components by the addition of Hg(II).

A number of studies have demonstrated that DOM originates from different sources, e.g., municipal solid waste (MSW) generated by households and commercial establishments, the effluent of treated wastewater and drinking water, express great variation in the composition and property in spectral signatures [15]. In present study, aromatic protein-like substances showed the maximum fluorescence intensity than those of other substances in raw DOM, which may be attributed to the microbial activity during aquaculture process.

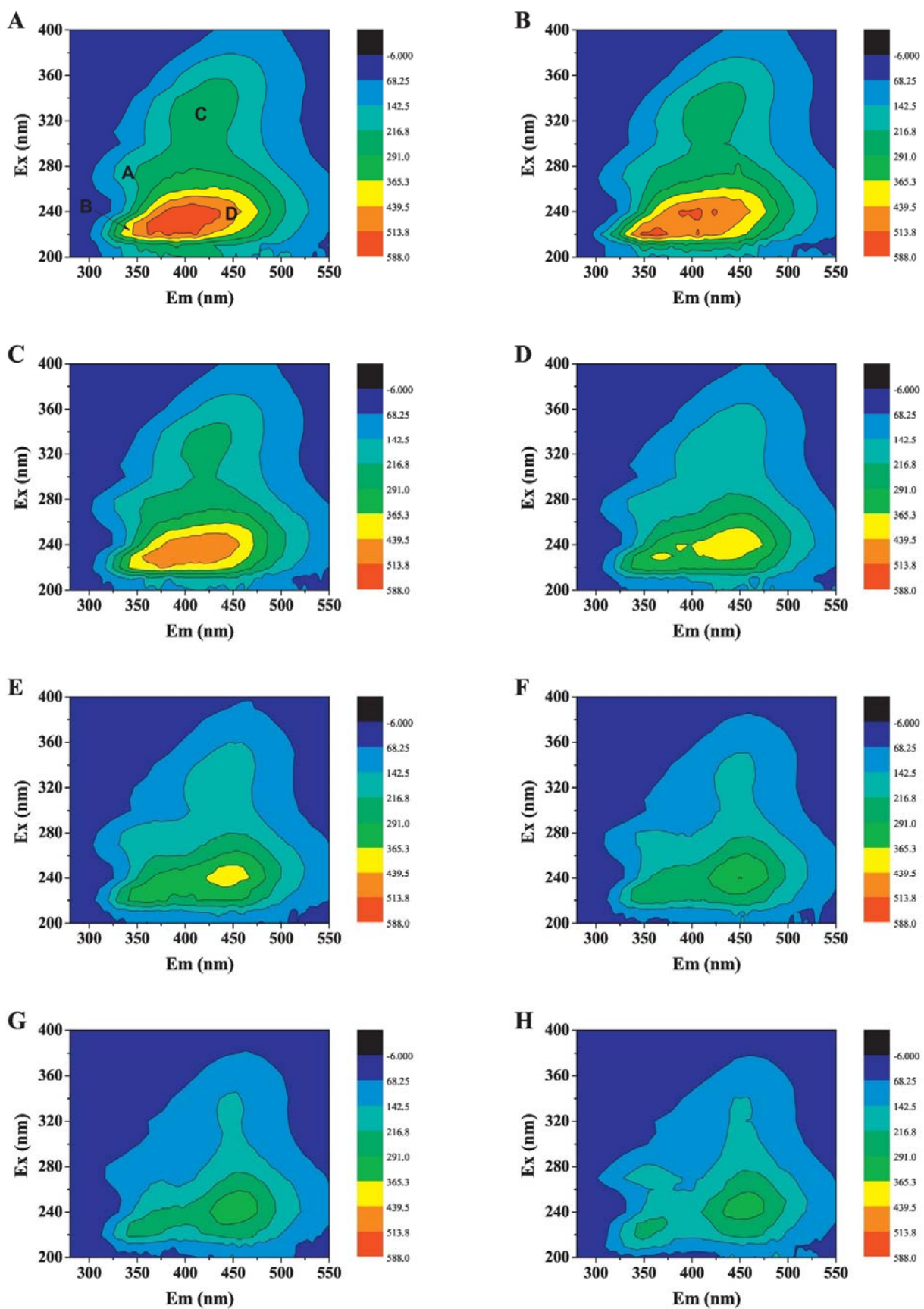


Fig. 1. 3D-EEM spectra of DOM samples interaction to various dosages of 4-CP: (A) 0 mg/L; (B) 0.7 mg/L; (C) 0.9 mg/L; (D) 2 mg/L; (E) 3 mg/L; (F) 4 mg/L; (F) 4.5 mg/L; (G) 5 mg/L.

Moreover, it has been reported that protein-like substances in the effluent of treated wastewater were more sensitive to the presence of toxic compound in aerobic granular sludge system [27]. Compared with DOM from aquaculture wastewater, the majority of DOM consisted of humic-like substances during the landfill process of MSW, which were much more difficult for the microorganisms to utilize than that of protein-like substances [28]. However, significant different fluorescent peaks were observed from clean reservoirs and rivers, including fulvic-like and humic-like substances, which may be derived from plant material [29]. In aquatic environment, humic acid substances play an important role on influencing the aggregation, surface affinity, and chemical behavior of clay minerals that influences the sorption of metal ions [30]. Moreover, it has also been reported that humic acid aggregates exhibited a negative surface potential in the presence of nuclide ion concentrations that affected the transportation and elimination of radionuclides [31].

Since various type of overlapping fluorophores in EEM spectra, PARAFAC analysis was applied to quantitative comparison of EEM through decomposing the complex EEM spectra into independent fluorescent components [32]. As shown in Fig. 2, two components of DOM were identified by PARAFAC model based on EEM spectra, and each component had two obvious fluorescent peaks. For component 1, one obvious fluorescent peak was identified at Ex/Em of 340/425.5 and 240/452.5 nm, which were ascribed to humic-like and fulvic-like substances [33]. Correspondingly, component 2 was characterized by one primary peak at Ex/Em of 270/362 nm and the secondary peak at Ex/Em of 220/356 nm, which were tryptophan protein-like substances and aromatic protein-like substances, respectively [34]. PARAFAC model also provides the relative scores of the two fluorescent components, which are related to their concentrations in the EEM dataset. It was found from Fig. 3 that the fluorescence intensity scores of two PARAFAC-derived components generally decreased with the addition of 4-CP, implying the interaction between various fluorescent components and organic matter.

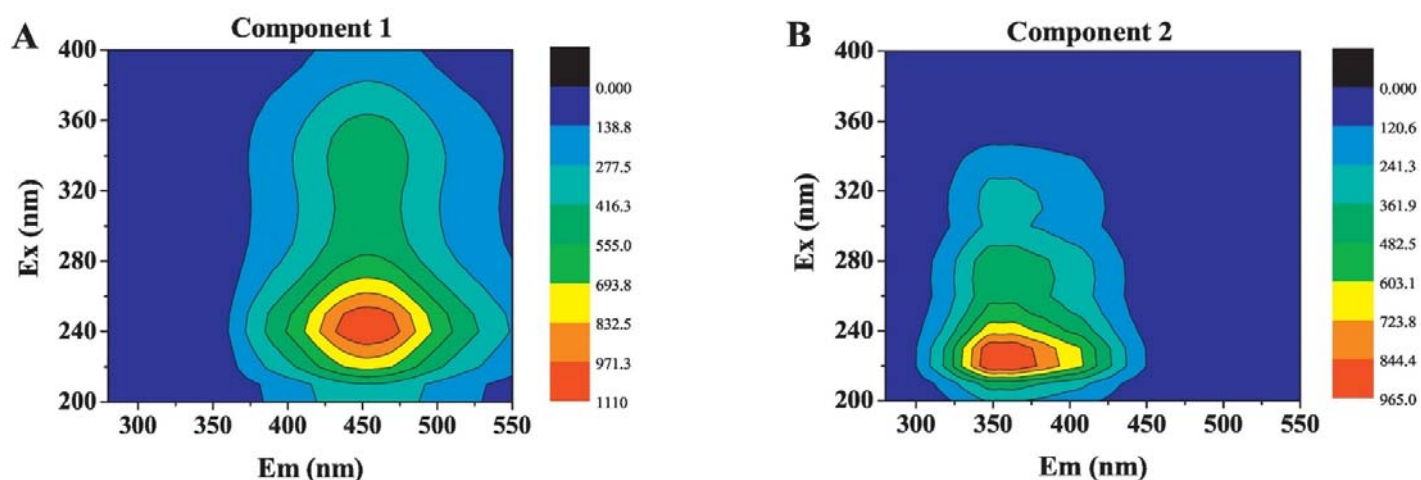


Fig. 2. Two components of DOM identified by PARAFAC based on EEM spectra: (A) Humic-like substances and fulvic-like substances; (B) Protein-like substances.

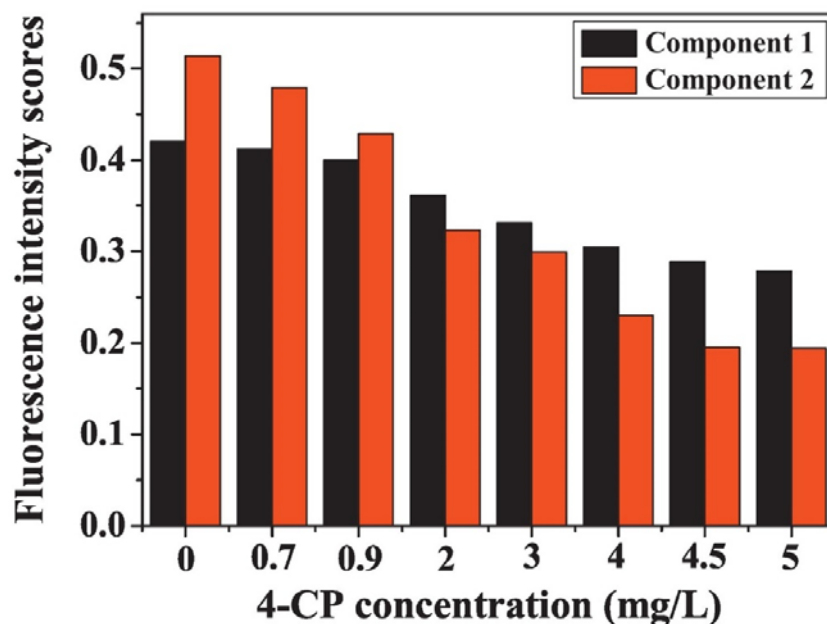


Fig. 3. Fluorescence intensity scores of two PARAFAC-derived components in eight DOM samples with increased 4-CP concentration.

3.2. Synchronous fluorescence spectra coupled with 2D-COS analysis

In present study, synchronous fluorescence spectra were recorded from solution of DOM at fixed concentration mixed with different 4-CP concentrations. Fig. 4 shows the changes in synchronous fluorescence spectra of DOM with increased 4-CP concentration. According to previous literature, three distinctive regions of synchronous fluorescence spectra were assigned to protein-like, fulvic-like, and humic-like fluorescence fractions, each of which corresponds to the integrated areas at wavelength of 250–300 nm, 300–380 nm and 380–550 nm, respectively [35]. As shown in Fig. 4, one broad peak and one small peak, centering at 281 and 338 nm, were observed in the synchronous fluorescence spectra of raw DOM. Overall wavelengths displayed a significant fluorescence quenching with similar spectral shape by the addition of 4-CP, suggesting the interaction between different fluorescent DOM fractions and 4-CP. Data implied that the two peaks reduced to the levels of 61.2% and 31.1% of the initial intensity of the raw DOM, respectively.

Fig. 5 shows the 2D-COS maps for the synchronous fluorescence spectra of interaction between DOM and 4-CP. In the 2D synchronous map (Fig. 5A), two major positive autopeaks were revealed at 284 nm and 338.5 nm along the diagonal line. The intensities of autopeaks decreased in the following order: 338.5 nm > 284 nm, suggesting that fulvic-like fraction might be more susceptible to 4-CP addition than that of protein-like fraction. In contrast, there were one broad and one small negative areas in upper the diagonal line of 2D asynchronous map (Fig. 5B). The two crosspeaks in the negative areas were centering at 284/338.5 nm and 284/388 nm. Based on Noda's rule, fluorescence quenching took place sequentially in the following order: 338.5 and 388 nm > 284 nm. The result implied that fluorescence quenching with increasing 4-CP concentration might occur preferentially in the order: fulvic-like and humic-like fractions > protein-like fraction. A similar quenching order in the copper bound to DOM fractions was also proved by Chen et al. [35], in

which the sequence was followed by humic-like fraction > fulvic-like fraction > protein-like fraction.

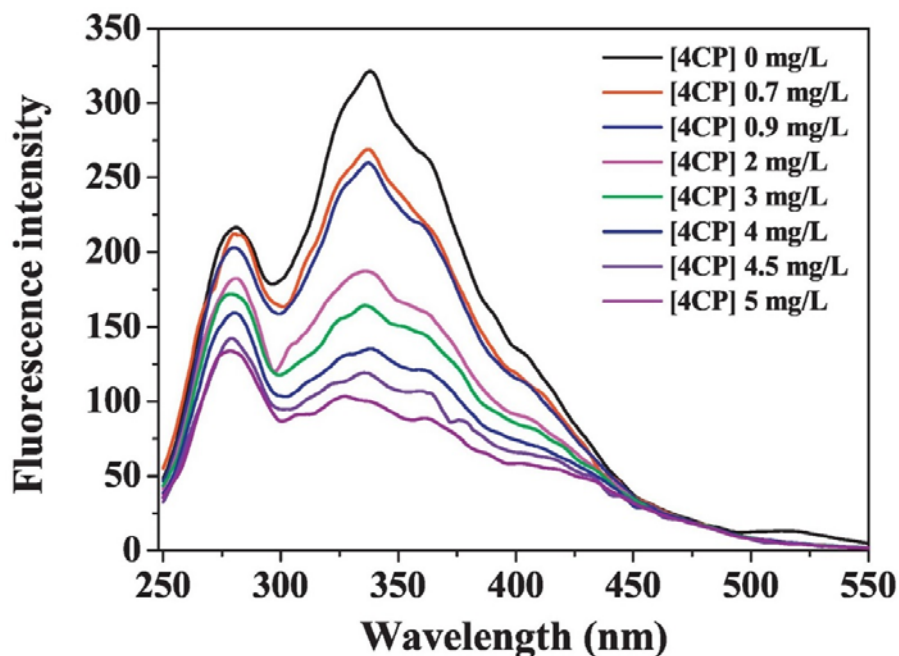


Fig. 4. Changes in synchronous fluorescence spectra of DOM with increased 4-CP concentration.

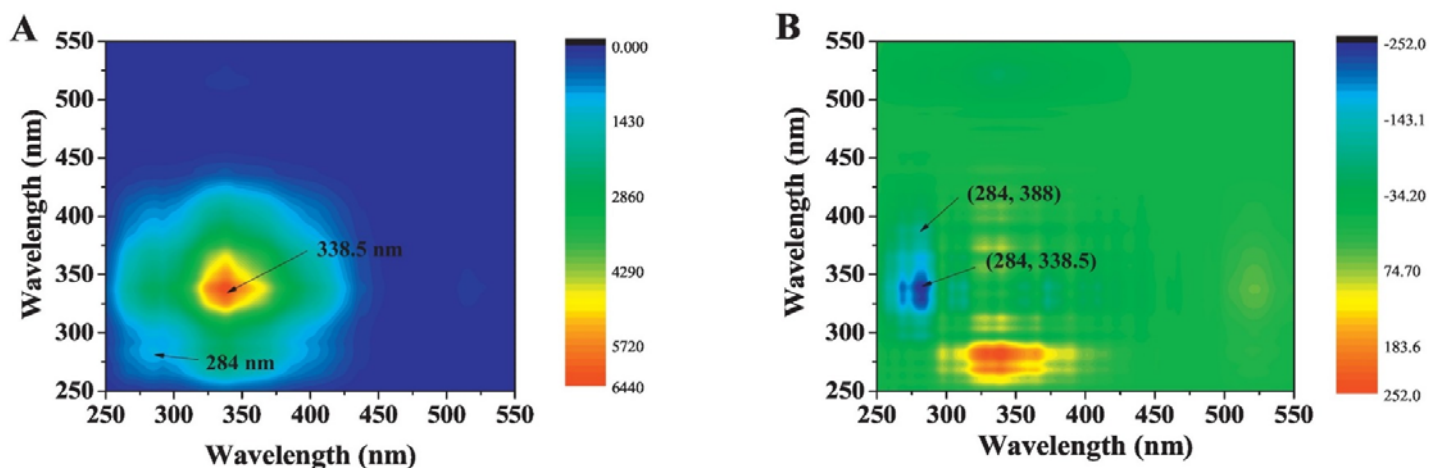


Fig. 5. 2D-COS maps for the synchronous fluorescence spectra of interaction between DOM and 4-CP: (A) synchronous map; (B) asynchronous map.

Since various types of nanomaterials have been widely produced and used in many applications that are existed in natural environment, therefore, the interactions between organic or inorganic pollutants (e.g. metal) and nanomaterials have also been well investigated via spectroscopic approaches [36,37]. Yu et al. [38] investigated the interaction of phenol and naphthol with reduced graphene oxide (rGO) by using FTIR and Raman, suggesting that a blue shift of C=C and -OH stretching modes and the enhanced intensity ratios of I_D/I_G after phenols sorption. Ren et al. [39] found that the interactions among graphene oxide (GO), Cd(II), and P(V) exhibited a significant

dependence on solution chemistry and addition sequences and these interactions subsequently affected the GO colloidal behavior.

3.3. Fluorescence quenching mechanism

Fluorescence quenching can occur by different mechanisms, which usually classified as dynamic quenching and static quenching. In order to confirm the quenching mechanism, three wavelengths at 284, 338.5 and 388 nm were selected in protein-like, fulvic-like and humic-like fractions from the 2D maps. The fluorescence decrease in intensity is described by the well-known Stern-Volmer equation (Eq. (3)):

$$F_0/F = 1 + K_{sv}[4\text{-CP}] = 1 + K_q\tau_0[4\text{-CP}] \quad (3)$$

where F_0 and F are the fluorescence intensities in the absence and presence of 4-CP, respectively, K_{sv} is the Stern-Volmer quenching rate constant, K_q is the biomolecular quenching rate constant, τ_0 is the average lifetime of the molecule in the absence of quencher (10^{-8} s), and $[4\text{-CP}]$ is 4-CP concentration.

Fig. 6A shows the Stern-Volmer plot of DOM with increased dosages of 4-CP. It was found that all the titration data were well fitted with the Stern-Volmer equation ($R^2 = 0.9166\text{--}0.9517$). The quenching rate constant of K_q for protein-like, fulvic-like and humic-like fractions were calculated as 1.78×10^{12} , 5.71×10^{12} and 3.77×10^{12} L/mol/s, respectively. All values were much higher than the value of maximum scatter collision quenching constant of quencher to biomacromolecule (2.0×10^{10} L/mol/s). Therefore, the fluorescence quenching of different DOM fractions to 4-CP may be initiated by complex formation rather than by dynamic collision.

For an interaction involving static quenching mechanism, the interaction constant (K_a) and the numbers of interaction sites (n) can be determined by the following equation (Eq. (4)):

$$\log \frac{F_0 - F}{F} = \log K_a + n \log [4\text{-CP}] \quad (4)$$

where F_0 , F and $[4\text{-CP}]$ are the same as in Eq. (1), the parameter K_a is the interaction constant, reflecting the reaction degree of fluorescent substances and 4-CP, and n is the number of interaction sites.

Fig. 6B shows the plot of $\log [(F_0 - F)/F]$ as a function of $\log [4\text{-CP}]$ for the interaction of DOM with 4-CP. It was found that the interaction constant (K_a) of protein-like, fulvic-like and humic-like fractions were 1.69×10^5 , 4.89×10^5 , 0.59×10^5 L/mol, respectively. The result implied that fulvic-like fraction in DOM had greater interaction capacity for 4-CP than that of protein-like fraction, which was consistent with the result of 2D-COS. Moreover, the numbers of interaction sites (n) of protein-like, fulvic-like and humic-like fractions for 4-CP interaction were 1.23, 1.22 and 1.05, respectively, suggesting that more than one class of interaction sites were present in the above fractions.

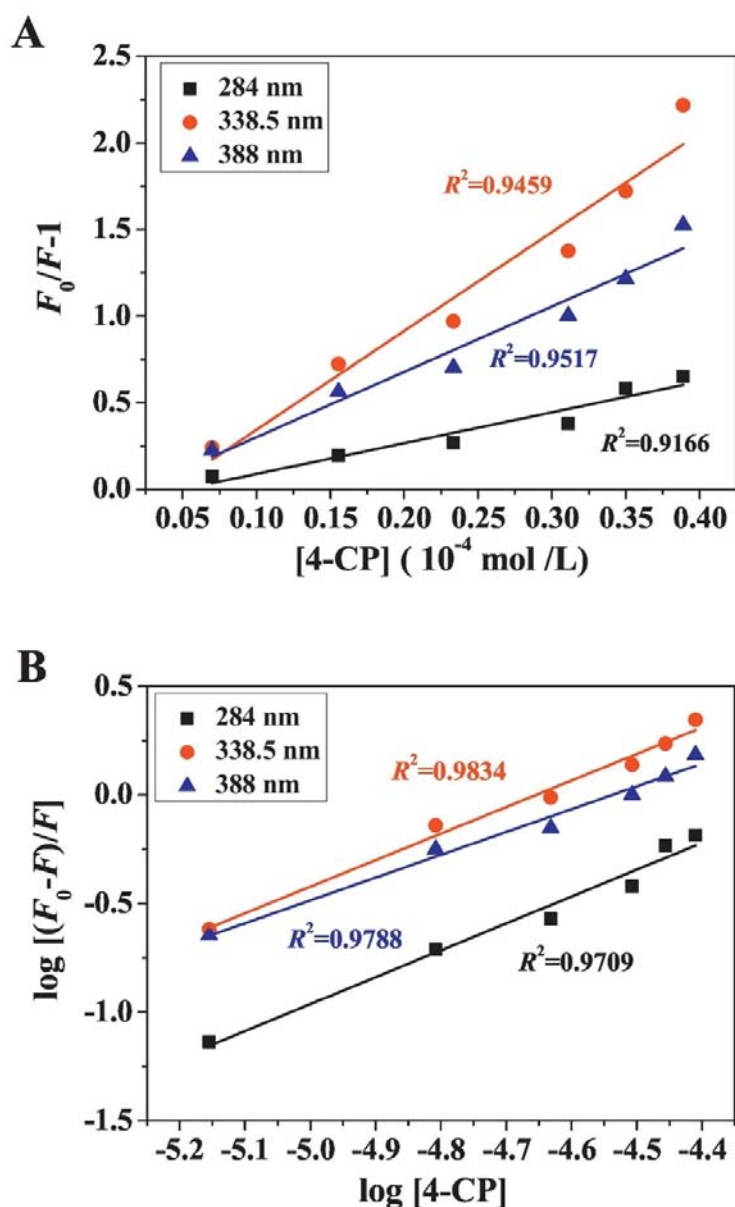


Fig. 6. (A) Stern-Volmer plot of DOM with increased dosages of 4-CP; (B) Plot of $\log[(F_0 - F)/F]$ as a function of $\log[4\text{-CP}]$ for the interaction of DOM with 4-CP.

3.4. FTIR

FTIR analysis was performed to identify the major functional groups in order to confirm the structural difference of DOM samples before and after interaction with 4-CP. It was found from Fig. 7 that the main functional groups of DOM samples expressed different characteristics in the presence and absence of 4-CP. For both samples, a strong and broad band approximately around $3421\text{--}3424 \text{ cm}^{-1}$ could be attributed to the overlap of O-H stretching of phenol, carbohydrate and carboxylic acid compounds, as similarly reported by Abdulla et al. [40]. The band at $1625\text{--}1628 \text{ cm}^{-1}$ represented the C=O stretching vibration of Amide I from protein [27]. A small band near 1396 cm^{-1} may be attributed to symmetrical stretching of --COO-- groups associated with amino acids. Two bands at 1116 and 620 cm^{-1} were assigned to the presence of C-O stretching of

aryl ethers/phenols and phosphate group, respectively [41]. It is clearly observed that the functional groups of DOM sample had small changes after interaction with 4-CP. The peak at 3423.5 cm^{-1} representing O–H stretching was shifted to 3421.6 cm^{-1} , while the peak at 1625.9 cm^{-1} representing the C=O stretching vibration of the functional groups was shifted to 1627.9 cm^{-1} . The shifted functional groups in DOM samples were the main contribution for interaction between DOM and 4-CP.

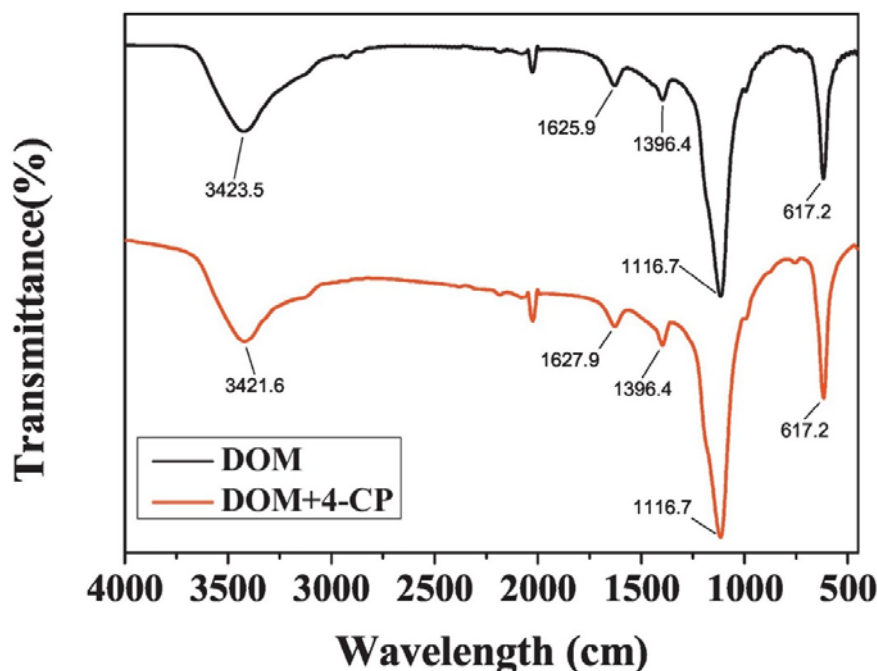


Fig. 7. Functional groups of DOM samples before and after interaction with 4-CP.

4. Conclusions

In summary, it was found from EEM-PARAFAC model identified two components from the interaction between DOM and 4-CP samples, including humic-like and fulvic-like substances for component 1 and protein-like substances for component 2, respectively. Synchronous fluorescence coupled with 2D-COS implied that the order of fluorescence quenching in DOM followed by fulvic-like and humic-like fractions > protein-like fraction. Moreover, all above fractions for 4-CP interaction process belonged to a static quenching mechanism. The main shifted functional groups were O–H stretching and C=O stretching vibration. The obtained result could provide a spectroscopic approach to assess the interaction between 4-CP and DOM from aquaculture wastewater.

Acknowledgements

This study was supported by the Key Research and Development Plan of Shandong Province (2018GSF117027), Natural Science Foundation of Shandong Province (ZR201702070162), National Natural Science Foundation of China (21777056, 51508226), A Project of Shandong Province Higher Educational Science and Technology Program (J17KA191), and QW thanks the

Special Foundation for Taishan Scholar Professorship of Shandong Province and UJN (No.ts20130937).

References

- [1] J. Nimptsch, S. Woelfl, S. Osorio, et al., *Sci. Total Environ.* 537 (2015) 129–138.
- [2] S. Sfez, D.H.S. Van, S.E. Taelman, M.S. De, J. Dewulf, *Bioresour. Technol.* 190 (2015) 321–331.
- [3] Z. Hu, J.W. Lee, K. Chandran, S. Kim, K. Sharma, A.C. Brotto 130 (2013) 314–320.
- [4] Z. Wei, X. Zhang, Y. Wei, X. Wen, J. Shi, J. Wu, *Bioresour. Technol.* 161 (2014) 179–185.
- [5] G.R. Aiken, H. Hsu-Kim, J.N. Ryan, *Sci. Technol.* 45 (2010) 3196–3201.
- [6] S. Hernandezruiz, L. Abrell, S. Wickramasekara, B. Chefetz, J. Chorover, *Water Res.* 46 (2012) 943–954.
- [7] K. Yamauchi, A. Ishihara, H. Fukazawa, Y. Terao, *Toxicol. Appl. Pharm.* 187 (2003) 110–117.
- [8] D. Wei, Y. Wang, X. Wang, M. Li, F. Han, L. Ju, G. Zhang, L. Shi, K. Li, B. Wang, *J. Hazard. Mater.* 289 (2015) 101–107.
- [9] W. Chen, X.Y. Liu, H.Q. Yu, *Environ. Pollut.* 222 (2017) 23–31.
- [10] T. Maqbool, J. Hur, *Chemosphere* 161 (2016) 190–199.
- [11] F.J. Rodríguez, P. Schlenger, M. García-Valverde, *Sci. Total Environ.* 476–477 (2014) 718–730.
- [12] M. Vera, S. Cruz, M.R. Boleda, et al., *Sci. Total Environ.* 584–585 (2017) 1212–1220.
- [13] X.S. He, B.D. Xi, X. Li, H.W. Pan, D. An, S.G. Bai, D. Li, D.Y. Cui, *Chemosphere* 93 (2013) 2208–2215.
- [14] B.J. Ni, R.J. Zeng, F. Fang, W.M. Xie, G.P. Sheng, H.Q. Yu, *Water Res.* 44 (2010) 2292–2302.
- [15] H.Y. Hu, D. Ye, Q.Y. Wu, Z. Xin, T. Xin, C. Zhuo, *Sci. Total Environ.* 551–552 (2016) 133–142.
- [16] J. Hur, B.M. Lee, *Chemosphere* 83 (2011) 1603–1611.
- [17] H. Xu, H. Jiang, *Water Res.* 47 (2013) 6506–6515.
- [18] H. Yu, Y. Song, X. Tu, E. Du, R. Liu, J. Peng, *Bioresour. Technol.* 144 (2013) 595.
- [19] D. Wei, M. Li, X. Wang, F. Han, L. Li, J. Guo, L. Ai, L. Fang, L. Ling, B. Du, Q. Wei, *J. Hazard. Mater.* 301 (2016) 407–415.
- [20] G.P. Sheng, J. Xu, H.W. Luo, W.W. Li, W.H. Li, H.Q. Yu, Z. Xie, S.Q. Wei, F.C. Hu, *Water Res.* 47 (2013) 607–614.
- [21] C.A. Andersson, *R. Bro.* 52 (2000) 1–4.
- [22] J. Hur, K.Y. Jung, Y.M. Jung, *Water Res.* 45 (2011) 2965–2974.
- [23] I. Noda, *Nova* 77 (2004) 239–244.
- [24] W. Chen, P. Westerhoff, J.A. Leenheer, K. Booksh, *Environ. Sci. Technol.* 37 (2003) 5701–5710.
- [25] Z. Wang, Z. Wu, S. Tang, *Water Res.* 43 (2009) 1533–1540.
- [26] D. Zhang, X. Pan, K.M.G. Mostofa, C. Xi, G. Mu, F. Wu, L. Jing, W. Song, J. Yang, Y. Liu, *J. Hazard. Mater.* 175 (2010) 359–365.
- [27] D. Wei, H. Dong, N. Wu, H.H. Ngo, W. Guo, B. Du, Q. Wei, *Sci Rep.* 6 (2016) 24444.
- [28] X.S. He, B.D. Xi, Z.M. Wei, Y.H. Jiang, C.M. Geng, Y. Yang, Y. Yuan, H.L. Liu, *Bioresour. Technol.* 102 (2011) 2322–2327.
- [29] H. Naomi, B. Andy, R. Darren, *River Res. Appl.* 23 (2007) 631–649.

- [30] L.Q. Tan, X.X.Wang, X.L. Tan, H.Y. Mei, C.L. Chen, T. Hayat, A. Alsaedi, T. Wen, S.S. Lu, X.K. Wang, *Chem. Geol.* 464 (2017) 91–100.
- [31] L. Tan, X. Tan, H. Mei, Y. Ai, L. Sun, G. Zhao, T. Hayat, A. Alsaedi, C. Chen, X. Wang, *Environ. Pollut.* 236 (2018) 835–843.
- [32] S.K.L. Ishii, T.H. Boyer, *Environ. Sci. Technol.* 46 (2012) 2006–2017.
- [33] S.B. Huang, Y.X.Wang, T. Ma, L. Tong, Y.Y.Wang, C.R. Liu, L. Zhao, *Sci. Total Environ.* 529 (2015) 131–139.
- [34] G.P. Sheng, H.Q. Yu, *Water Res.* 40 (2006) 1233–1239.
- [35] W. Chen, N. Habibul, X.Y. Liu, G.P. Sheng, H.Q. Yu, *Environ. Sci. Technol.* 49 (2015) 2052–2058.
- [36] X. Liu, J. Li, Y. Huang, X.Wang, X. Zhang, *Environ. Sci. Technol.* 51 (2017) 6156–6164.
- [37] Y. Zou, X.Wang, A. Khan, P.Wang, Y. Liu, A. Alsaedi, T. Hayat, X.Wang, *Environ. Sci. Technol.* 50 (2016) 7290–7304.
- [38] S. Yu, X.Wang, W. Yao, J.Wang, Y. Ji, Y. Ai, A. Alsaedi, X.Wang, *Environ. Sci. Technol.* 51 (2017) 3278–3286.
- [39] X. Ren, Q.Wu, H. Xu, D. Shao, X. Tan, W. Shi, C. Chen, J. Li, Z. Chai, T. Hayat, X.Wang, *Environ. Sci. Technol.* 50 (2016) 9361–9369.
- [40] H.A.N. Abdulla, E.C. Minor, R.F. Dias, P.G. Hatcher, *Geochim. Cosmochim. Acta* 74 (2010) 3815–3838.
- [41] H.W. Wang, X.Y. Li, Z.P. Hao, Y.J. Sun, Y.N. Wang, W.H. Li, Y.F. Tsang, *J. Environ. Manag.* 191 (2017) 244–251.